

Experimental investigation of SRHSC columns under biaxial loading

Peng Wang*, Qing X. Shi^a, Feng Wang^b and Qiu W. Wang^a

School of Civil Engineering, Xi'an University of Architecture & Technology, No.13, Yanta Road, Xi'an, Shaanxi, China

(Received January 15, 2017, Revised December 24, 2017, Accepted December 26, 2017)

Abstract. The behavior of 8 steel reinforced high-strength concrete (SRHSC) columns, which comprised of four identical columns with cross-shaped steel and other four identical columns with square steel tube, was investigated experimentally under cyclic uniaxial and biaxial loading independently. The influence of steel configuration and loading path on the global behavior of SRHSC columns in terms of failure process, hysteretic characteristics, stiffness degradation and ductility were investigated and discussed, as well as stress level of the longitudinal and transverse reinforcing bars and steel. The research results indicate that with a same steel ratio deformation capacity of steel reinforced concrete columns with a square steel tube is better than the one with a cross-shaped steel. Loading path affects hysteretic characteristics of the specimens significantly. Under asymmetrical loading path, hysteretic characteristics of the specimens are also asymmetry. Compared with specimens under unidirectional loading, specimens subjected to bidirectional loading have poor carrying capacity, fast stiffness degradation, small yielding displacement, poor ductility and small ultimate failure drift. It also demonstrates that loading paths affect the deformation capacity or deformation performance significantly. Longitudinal reinforcement yielding occurs before the peak load is attained, while steel yielding occurs at the peak load. During later displacement loading, strain of longitudinal and transverse reinforcing bars and steel of specimens under biaxial loading increased faster than those of specimens subjected to unidirectional loading. Therefore, the bidirectional loading path has great influence on the seismic performance such as carrying capacity and deformation performance, which should be paid more attentions in structure design.

Keywords: steel reinforced concrete columns; high-strength concrete; bidirectional loading; coupling effect; seismic behavior

1. Introduction

Columns are key structural elements for seismic performance of the buildings. Therefore, special attention should be given to their structural response under load reversals. Although the response characteristics of columns under monotonic and unidirectional lateral cyclic loading are well understood, seismic excitations are not unidirectional but bidirectional in nature. Earthquake effects generally require the inclusion of two horizontal component loads that are recognized to be more damaging than single direction actions (Rodrigues *et al.* 2013a). Previous studies have been mostly focused on seismic behavior of members under uniaxial loading, while few studies of columns under biaxial cyclic moments are conducted. Our present-day knowledge of inelastic performance of columns under bidirectional cyclic loading is much limited and incomplete than our understanding of their behavior under uniaxial cyclic loading with an axial load.

Among those limited researches, the effects of proportional biaxial bending had been studied by Warner (1969), Farah and Huggins (1969), Mavichak and Furlong (1976), Furlong (1979), Poston *et al.* (1985a, b), Wang and

Hsu (1992, 1998), Ahmad and Weerakoon (1995) and Chang (2010). Rodrigues *et al.* (2012a, 2013b, c) carried out experimental studies of full-scale quadrangular reinforced concrete (RC) columns under unidirectional and bidirectional loading conditions. The test results indicate that for biaxial loading conditions specific damage occurs for lower drift demands when compared with the corresponding uniaxial demand (a reduction of 50-75% was found). No significant differences were found in the plastic hinge length for uniaxial and biaxial loading. Rodrigues *et al.* (2016) also found that biaxial loading can introduce higher energy dissipation than uniaxial loading, however, this fact was not clearly observed in columns under varying axial load. Otani *et al.* (1977) tested RC columns under cyclic multi-axial loading. Uniaxial loading, diagonal loading and square-shape loading on the top ends of columns were adopted in the test. Bousias *et al.* (1995) conducted the experiment of twelve identical flexure-dominated RC columns to study their seismic behavior under cyclic biaxial flexure with axial load focused on the effect of load path on behavior. It was found that very strong coupling was observed between the two directions of bending and between these two directions and the axial direction. Muñoz and Hsu (1997) studied the behavior of four small-scale concrete-encased I-shape steel columns subjected to biaxial bending moments and axial compressive load experimentally. Different finite methods were used to establish the relationship between curvature and deflection. Dundar *et al.* (2008) tested many RC and

*Corresponding author, Ph.D.

E-mail: wangpeng870822@163.com

^aPh.D.

^bPh.D. Student

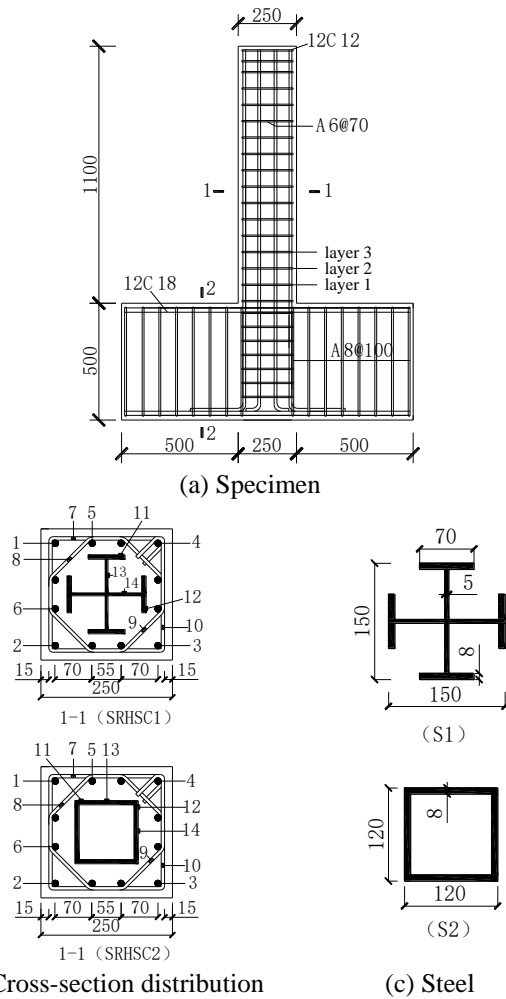


Fig. 1 Design details for SRHSC specimens

concrete-encased composite columns subjected to biaxial bending and axial load. And an iterative numerical procedure for strength analysis and design of reinforced concrete and concrete-encased composite columns under biaxial bending and axial load was proposed. Qiu *et al.* (2002) tested seven RC specimen columns under biaxial loading with different loading paths independently and concluded that bidirectional loading was found to weaken biaxial strength and hysteretic energy dissipation capacity. The experiment of two RC columns with rectangular cross-section was carried out under cyclic biaxial loading by Tsuno and Park (2004), Bechtoula *et al.* (2005) tested eight large scale and eight small-scale RC columns under various vertical and horizontal loading patterns. From the test observations, bidirectional loading had a great influence on the envelope curves as well as on damage development. An analytical model for prediction of the load carrying capacity of CFRP-confined columns under uniaxial and biaxial eccentric loading was proposed by Sayed and Maaddawy (2011). Quang *et al.* (2016) studied behavior of high-performance fiber-reinforced cement composite columns subjected to biaxial and axial loads experimentally. The test results demonstrated that biaxial loading tended to reduce the maximum strength degradation, and ductility of the specimen was decreased when increased axial load. Sixteen

full-scale steel fiber reinforced concrete cantilever columns were tested under cyclic uniaxial and biaxial loading plus constant axial load by Germano *et al.* (2016), and the result indicated that biaxial loading turned out as a more severe load condition than the uniaxial one, reducing the ultimate displacement capacity, available ductility and energy dissipation. Krzysztof and Winnicki (2016) conducted experimental research and analysis of load capacity and deformability of slender high strength concrete columns under biaxial bending. Based on uniaxial models, a simplified interaction model for the response of RC columns under biaxial loading is proposed by Rodrigues *et al.* (2012b). And the validity of the proposed model was demonstrated through the analytical simulation of biaxial tests on RC columns. A simple efficient theoretical method was proposed for estimating the strength of short and slender RC columns under axial load and biaxial bending by Hong (2000, 2001). de Sousa and Caldas (2005) presented a numerical formulation for the nonlinear analysis of slender steel-concrete composite columns of generic cross-sectional shape subjected to axial force and biaxial bending. Numerical analyses were conducted to study the effects of bidirectional lateral cyclic loading on hysteretic response of stocky circular thin-walled steel columns by Ucak and Tsopelas (2015). Four unidirectional and eight bidirectional lateral displacement controlled load paths were considered. The results indicated that bidirectional lateral cyclic loading had a very limited effect on the ultimate strength of stocky circular thin-walled steel columns, but significantly decreases the ductility when compared with unidirectional lateral loading. In addition, behavior of columns with T-, L- and cross-shaped cross sections were studied under bidirectional bending by Hsu (1985, 1989) and Tokgoz and Dunder (2008).

Compared with studies of uniaxial behavior of columns, experimental research on the inelastic response of columns under biaxial lateral cyclic bending load is currently very limited. As for the research of biaxial response of members carried out before, they mainly focused on reinforced concrete columns and reinforced concrete special-shaped

Table 1 Experimental parameters of specimens

Specimen	Load-path	Steel configuration	Steel ratio (%)	Test axial load ratio n	Transverse reinforcing bars	Longitudinal reinforcing bars
SRHSC1-B0	B0	S1	5.69	0.35	$\phi 6@70$	$12\phi 12$
SRHSC2-B0	B0	S2	5.57	0.35	$\phi 6@70$	$12\phi 12$
SRHSC1-B1	B1	S1	5.69	0.35	$\phi 6@70$	$12\phi 12$
SRHSC2-B1	B1	S2	5.57	0.35	$\phi 6@70$	$12\phi 12$
SRHSC1-B2	B2	S1	5.69	0.35	$\phi 6@70$	$12\phi 12$
SRHSC2-B2	B2	S2	5.57	0.35	$\phi 6@70$	$12\phi 12$
SRHSC1-B3	B3	S1	5.69	0.35	$\phi 6@70$	$12\phi 12$
SRHSC2-B3	B3	S2	5.57	0.35	$\phi 6@70$	$12\phi 12$

Table 2 Properties of steel and reinforcing bars

Material	Strength grade	Diameter (Plate thickness)/mm	Yield strength f_y /MPa	Ultimate strength f_u /MPa	Elongation δ_u /%	Elastic modulus E_s /10 ⁵ MPa
Reinforcing bars	HPB235	6.6	324.87	451.43	27	2.24
	HPB235	8.3	341.23	440.72	21	2.36
	HRB400	11.2	394.43	612.88	28	1.92
	HRB400	17.4	363.91	563.08	33	1.98
Steel plates	Q235	4.6	290.64	431.18	35	2.13
	Q235	7.2	279.15	423.62	32.5	1.93
Square steel tube	Q235	7.75	280.20	445.56	34	2.03

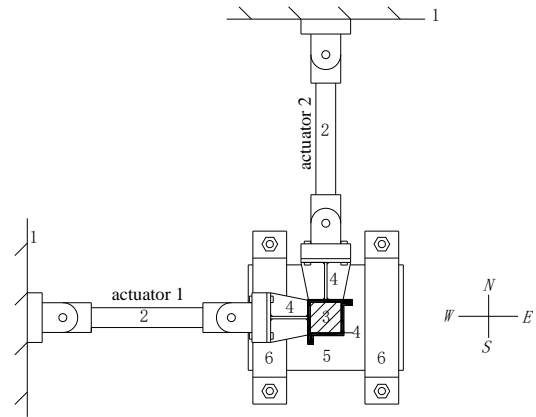
columns. Few studies of steel reinforced concrete (SRC) and steel reinforced high-strength concrete (SRHSC) columns subjected to bidirectional loading are conducted, and the biaxial response of SRC and SRHSC columns is still far from being well understood.

This paper contributes to further understanding of seismic behavior of SRHSC columns subjected to biaxial loading. An experimental program was carried out on eight steel reinforced concrete columns under lateral cyclic load and constant axial load. Both unidirectional and bidirectional lateral displacements were imposed in order to better simulate the actual response of a column during an earthquake. The variable parameters in test specimens were loading paths and layout of steel. The behavior of specimens was discussed in terms of crack pattern, hysteretic response, ductility, energy dissipation capacity and strain of reinforcement. By contrast, the biaxial response of SRHSC columns was studied in the paper.

2. Experimental program

2.1 Description of test specimens

Eight 1/4-scale cantilever-type SRHSC columns, which comprised of four identical columns with cross-shaped steel and other four identical columns with square steel tube, were fabricated and tested under a combination of constant axial load and uniaxial or biaxial cyclic lateral load. All columns were designed to have a same cross section of 250 mm×250 mm. And the clear height of specimens was set to be 1000 mm, resulting in an aspect ratio of $\lambda=4$. Design details of the columns are shown in Fig. 1 and Table 1. Test specimens were cast vertically using fine aggregate commercial high-strength concrete having a design axial compressive strength of 25.3 MPa at 28 days. Grade Q235 steel was used in all specimens with a design yielding strength of 215 MPa. And they had a steel ratio of about 5.7%. The longitudinal reinforcement was made up of 12 ϕ 12 (diameter $d=12$ mm) steel bars with a design yielding strength of 360 MPa, and the ratio of longitudinal reinforcement was 2.17%. These steel bars were evenly distributed on all cross-sections of the column, which had a concrete cover of 15 mm. Composite transverse reinforcement, which consisted of $\phi 6$ (diameter $d=6$ mm) stirrups with a design yielding strength of 270 MPa and a



1. Reaction wall. 2. 1000kN horizontal actuator. 3. Specimen. 4. Biaxial loading connector. 5. The base of specimen. 6. Fixing device.

Fig. 2 Test setup

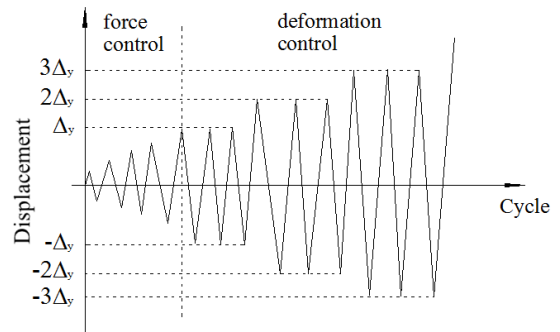


Fig. 3 Loading procedure

vertical spacing of 70 mm, was used for all the specimens, and the volume stirrup ratio was 1.52%. Design of the specimens was satisfied with GB 50011-2010 (2010). The properties of steel and reinforcing bars are tabulated in Table 2.

2.2 Testing procedure

Low cyclic loading was applied to each specimen while axial compression was held constant. The test setup is shown in Fig. 2. A spherical hinge was used to maintain the boundary condition of free rotation at the top of the specimen during test. Two orthogonal horizontal actuators were used to provide lateral load. The lateral load was applied cyclically through the horizontal actuator in a quasi-static fashion, as shown in Fig. 3. Load-displacement hybrid control program was applied, in which the lateral loading sequence was controlled by force for the initial loading cycles till the yielding initiation of the test specimen was observed. This observation was accomplished by monitoring the reaction force of the MTS horizontal actuator. From 30 kN, every load level was applied for 1 cycle in an increment of 30 kN. When loaded to the yielding force, the loading sequence was controlled by displacement. Then, the target displacement for the cyclic loading was set as the multiple of the yield displacement (Δ_y), and it was repeated three times at each displacement level. Refer to the literatures composed by Kang *et al.*

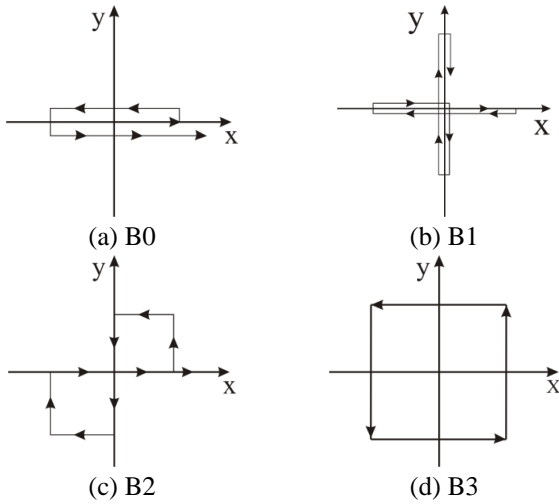


Fig. 4 Load-path on the top end of the specimen

(2003), Rodrigues *et al.* (2016), Qiu *et al.* (2002), one uniaxial load-path and three biaxial load-paths, as shown in Fig. 4, are chosen and applied in the test. The test was terminated until the reaction force descended to about 70% of the maximum load.

2.3 Instrumentations

The test specimens had been extensively installed with measuring devices both internally and externally. Lateral displacements in the *x*- and *y*-direction were measured by two horizontal LVDTs parallel to each horizontal actuator, respectively. And they were mounted at the top side of specimen columns. Shear and flexural deformation were obtained by readings of a number of LVDT sets mounted throughout the height of the specimens. Strain gauges were mounted to capture the strain history in steel plates, longitudinal reinforcing bars and stirrups at critical positions, as shown in Fig. 1.

3. Specimen behavior

3.1 Cracking pattern

Since all specimen columns were designed in flexure-dominated, a flexure failure was found in all specimens. Fig. 5 gives the cracking patterns of specimens, in which the dimensions of square grid are 50 mm×50 mm. In the figures, “positive sign” and “negative sign” represent the force or displacement in the push and pull directions, respectively. In front of the “sign”, “1” and “2” stand for the actuator 1 and the actuator 2, respectively. And there is no number for the specimen subjected to uniaxial cyclic loading. “*i*” represents ton for short, and the front number is the peak lateral load for the loading cycle. “Δ” stands for the yielding displacement, and the front number is the multiple of the yielding displacement, while the latter number is the times of loading cycles for one certain displacement level. It was found that the cracks of specimens were mainly developed horizontally in the

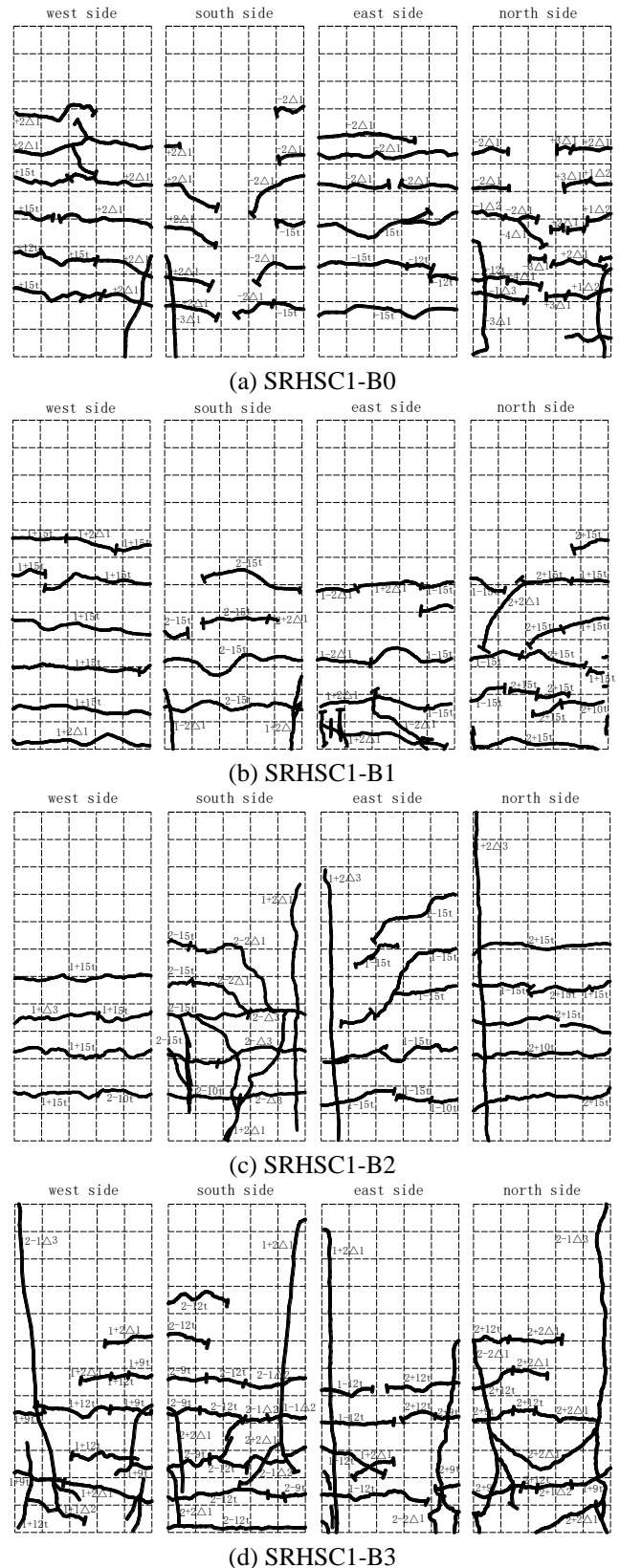


Fig. 5 Cracking pattern of specimens

plastic hinge field, while vertical split cracks were few and they happened in the corner of the specimens generally. Cracking development differed due to different loading path. The cracking process of specimens under various

forms of loading is as follows.

Specimen SRHSC1-B0

Specimen SRHSC1-B0 was tested under uniaxial cyclic lateral load and constant axial load. When loaded to 120 kN, horizontal cracks were observed in east and west sides of the specimen, which were approximately 160 mm and 180 mm away from bottom end of the column, respectively. Under an approximate load of 150 kN, the existing cracks extended and some new horizontal cracks happened in the east and west sides. These cracks spread slantingly in the south and north sides. Furthermore, three cracks of the east side developed into horizontal penetrating cracks in the plastic hinge field. Under cyclic loading of $2\Delta_y$ (Δ_y was the yield displacement), a few existing cracks in west side developed and formed into pass-through cracks. And there were also many new horizontal pass-through cracks emerging in east and west sides. Slight vertical split cracks happened in southwest- and southeast corners of the specimen column. When loaded to $3\Delta_y$, the existing cracks had almost no extending, however, some cover concrete started to spalling. Under cyclic loading of $4\Delta_y$, the width of main cracks increased. However, there was almost no new crack emerging. Large-area cover concrete started to spall. Under cyclic loading of $5\Delta_y$, cover concrete located at flexural hinge zone was spalling severely. Some transverse reinforcements were exposed after cover concrete spalling. And longitudinal steel bars were buckling at the plastic field. Cracking development and cover concrete spalling mainly happened in east and west side during the loading test.

Specimen SRHSC1-B1

Specimen SRHSC1-B1 was tested subjected to biaxial cyclic lateral load B1 and constant axial load. The cracking load was about 100 kN. A tiny crack was observed in the north side and developed horizontally. When loaded to 150 kN, yielding of longitudinal reinforcing bars was observed. Many cracks formed in all sides and two cracks developed to be pass-through cracks, where were about 80 mm and 150 mm away from the bottom column end, respectively. At the same time, a long tiny crack occurred at the bottom column end and developed horizontally. When the lateral displacement reached to $2\Delta_y$ and was repeated 3 times, there were almost no new cracks emerging. The width of existing cracks increased. A tiny vertical split crack formed at southeast corner of the specimen. Moreover, large area cover concrete started to spalling. When loaded to $3\Delta_y$, the corner concrete split severely. Meanwhile, there was large cover concrete spalling at the east, south and north sides.

Specimen SRHSC1-B2

Specimen SRHSC1-B2 was tested subjected to biaxial cyclic lateral load B2 and constant axial load. When loaded to 100 kN, tiny cracks occurred in all sides of the specimen, the one of the north side developed to be a pass-through crack. When the lateral load reached to 150 kN, many new cracks formed in all sides of the specimen. And the existing cracks developed horizontally into pass-through cracks. Also a slight vertical split crack was observed at southeast corner of the specimen column. Under a lateral loading of $2\Delta_y$, large cover concrete crushed and dropped at east side of the specimen. And large vertical split cracks occurred in

southeast- and northeast corner of the specimen during the cyclic loading. When the lateral displacement reached to $3\Delta_y$, the existing split cracks developed severely. Cover concrete dropping from plastic hinge field of the specimen increased continuously and severely. After cover concrete dropping, a great number of transverse reinforcement and longitudinal reinforcing bars were exposed.

Specimen SRHSC1-B3

Specimen SRHSC1-B3 was tested subjected to biaxial cyclic lateral load B3 and constant axial load. The cracking load was 90 kN. Cracks were tiny and developed horizontally at corner of the specimen. When loaded to 120 kN, the existing cracks extended, more flexural cracks were observed and tiny vertical split cracks occurred at northwest and northeast sides of the specimen. When the lateral displacement reached to $2\Delta_y$, a few new cracks formed and the existing cracks extended slightly. A large vertical split crack was observed and its split height was about 550 mm. When the lateral displacement reached to $3\Delta_y$, cover concrete crushed and dropped all around the plastic hinge field. Under a lateral displacement of $4\Delta_y$, cover concrete crushed and dropped severely in all sides of the specimen. After cover concrete spalling, transverse and longitudinal reinforcement were exposed and the longitudinal reinforcements were buckling in the plastic field.

From the cracking pattern mentioned above, it is found that loading path has little effect on the cracking load of SRHSC columns. Specimens had longer length of flexural cracking field along the axial direction under uniaxial cyclic loading than biaxial cyclic loading. Moreover, their damage mainly happened at two sides that were perpendicular to the lateral loading direction. As for the specimen subjected to biaxial cyclic loading, cracking development and cover concrete spalling occurred rapidly, especially in the case of specimens subjected to loading paths B2 and B3. And their vertical split height of cracks was significantly larger than those specimens subjected to uniaxial cyclic loading.

3.2 Hysteretic response

Generally, hysteretic response illustrates the pinching effect, stiffness degeneration, and strength reduction during repeated cyclic loading, and it is an important index to measure the energy dissipation of earthquake resistant members and structures. Hysteretic responses obtained from the test are depicted in Fig. 6. From Fig. 6, it can be seen that specimens had some hysteretic characteristics in common. Before reaching the yielding load, hysteretic curves of all specimens were narrow, with poor energy dissipation and no significant stiffness degradation. When unloaded to the initial loading position, the residual deformation of specimens was very little. After the yielding load was attained, with the increasing area of hysteretic loops, energy dissipation started increasing. Compared specimens under biaxial cyclic loading with those subjected to uniaxial cyclic loading, it was found that the shape and plumpness of hysteretic curves differed greatly among specimens subjected to various loading paths. For example, columns under loading path B2 and B3 had a more plump hysteretic curve than the one under loading path B1.

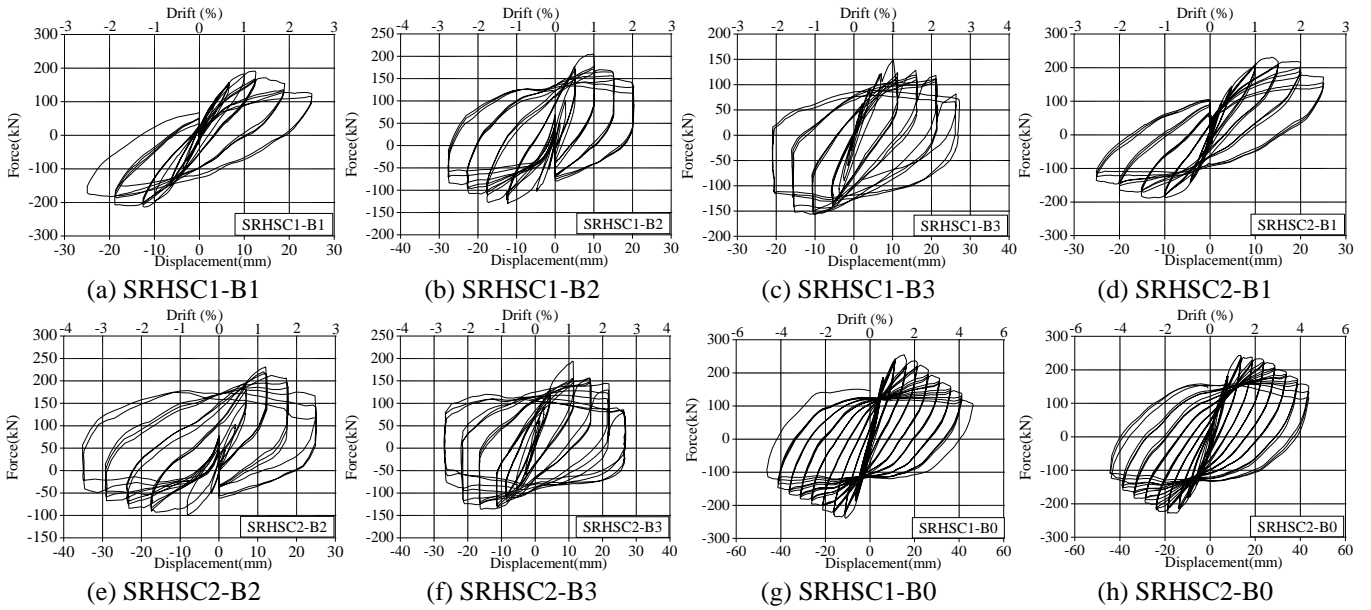


Fig. 6 Hysteretic curves of specimens under different loading paths in the x direction

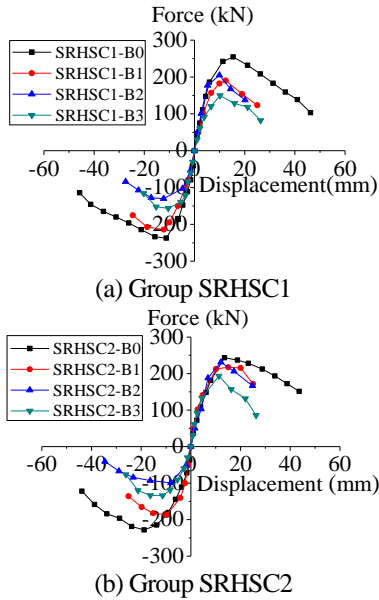


Fig. 7 Backbone curves of specimens

Moreover, the specimen subjected to biaxial cyclic loading had a sudden strength loss after the maximum lateral load attained, especially in the case of those under loading paths B2 and B3. And at a same level of cyclic loading, carrying capacity of biaxially loaded columns during the last two cycles decreased more severely than that of specimens subjected to axial loading. It indicates that cyclic loading imposed on specimens in one direction also has great influence on seismic character of specimens in the other direction. Result implies that columns exhibit significant coupling effect between two lateral loading directions.

3.3 Backbone curves

Backbone curves obtained from test are shown in Fig. 7. It is found that loading path has significant effect on

Table 3 Strength decrease of specimens subjected to biaxial cyclic loading

Specimen	Positive direction (push)		Negative direction (pull)	
	Force (kN)	Reduction ratio	Force (kN)	Reduction ratio
SRHSC1-B0	254.7	—	-237.5	—
SRHSC1-B1	190.6	25.2%	-213.9	9.9%
SRHSC1-B2	205.0	19.5%	-130.2	45.2%
SRHSC1-B3	149.5	41.3%	-156.4	34.2%
SRHSC2-B0	243.5	—	-228.2	—
SRHSC2-B1	217.3	10.7%	-186.9	18.1%
SRHSC2-B2	231.2	5.0%	-99.2	56.5%
SRHSC2-B3	193.4	20.6%	-134.3	41.1%

strength of specimens. Strength loss of specimens subjected to biaxial cyclic loading is tabulated in Table 3. It was easily found that strength were decreased by an average of 17.55%, 21.57% and 37.75% in the positive and negative directions for specimen SRHSC1-B1, SRHSC1-B2 and SRHSC1-B3, respectively. And there were 14.40%, 30.75% and 30.85% reduction for specimen SRHSC2-B1, SRHSC2-B2 and SRHSC2-B3, respectively. Specimens had much little yielding displacement subjected to biaxial cyclic loading than uniaxial cyclic loading. The reduction ratio of yielding drifts is tabulated in Table 4. Average reductions of yielding displacement for specimens SRHSC1 and SRHSC2 were 15.04% and 22.28%, respectively. Thus, the test results indicate that for biaxial loading conditions yielding occurs for lower lateral drift demands when compared with the corresponding uniaxial demand. Moreover, strength reduced rapidly after the maximum load attained in those specimens subjected to biaxial cyclic

Table 4 Reduction ratio of yielding drifts for specimens subjected to biaxial cyclic loading

Specimen	Positive direction (push)		Negative direction (pull)	
	Yielding drift (mm)	Reduction rate	Yielding drift (mm)	Reduction rate
SRHSC1-B0	9.2	—	-8.1	—
SRHSC1-B1	7.9	14.1%	-8.4	-4.2%
SRHSC1-B2	6.2	32.2%	-7.6	5.4%
SRHSC1-B3	7.5	18.7%	-7.7	4.8%
SRHSC2-B0	10.7	—	-10.5	—
SRHSC2-B1	7.9	25.7%	-7.6	27.3%
SRHSC2-B2	9.3	12.8%	-7.9	25.0%
SRHSC2-B3	8.0	24.7%	-8.6	18.2%

loading.

In addition, what can be easily found is that hysteretic character exhibits evident asymmetry for specimens subjected to asymmetric loading path B2. The peak load was much larger in the positive direction than in the negative direction. It should be caused by the asymmetry of loading path B2. Regarding to loading path B2, loading was firstly carried out on specimens in the *x* direction. Then, loading was conducted in the *y* direction while displacement in the *x* direction was held constant. Hence, damage firstly happened in both sides of specimens of *y* axis, carrying capacity of specimens was much little in the negative *x* direction than in the positive *x* direction.

3.4 Ductility

Ductility illustrates deformation capacity of structure

component after reaching the peak lateral force. In this paper ductility coefficient and damage drift ratio were taken to describe deformation capacity of the test specimens. Computational expressions are as follows

$$\mu_{\Delta} = \Delta_d / \Delta_y \quad (1)$$

$$\theta_d = \Delta_d / H \quad (2)$$

Where μ_{Δ} is ductility coefficient, θ_d is damage drift ratio, Δ_d is damage displacement, Δ_y is yielding displacement, and *H* is clear height of the specimen. The yielding lateral force was defined by monitoring the MTS horizontal actuator and the yielding displacement is the displacement at the yielding force. The damage displacement is the one where 85% of peak lateral load is sustained.

The displacement, drift ratio and corresponding force of specimens under critical stages are shown in Table 5. (“positive value” and “negative value” represents the force or displacement in the push and pull directions, respectively.). It was found that the drift ratios were 1/116 and 1/94 for specimens SRHSC1-B0 and SRHSC2-B0 when loaded to yielding, while the ultimate damage drift ratios were 1/41 and 1/33 respectively. By contrast with specimen SRHSC1-B0, the yielding drift ratio and ultimate drift ratio of specimen SRHSC2-B0 were increased by 23.40% and 24.24% respectively. It indicates that with a same steel ratio deformation capacity of SRHSC columns with square steel tubular is superior to that of SRHSC columns with cross-shape steel.

Compared columns under bidirectional loading with those subjected to unidirectional loading, the lateral drift ratios were decreased by 12.42%, 15.58% and 29.30% for specimen group SRHSC1 when loaded to yielding, ultimate strength and ultimate damage, and they were 22.40%, 25.30% and 31.78% for specimen group SRHSC2. Furthermore, the damage drift ratio was 1/41 for SRHSC1-B0, while the damage drift ratios were 1/59, 1/57 and 1/58

Table 5 Test results of specimens under different loading stages in the *x* direction

Specimen	Loading direction	Yielding			Ultimate strength			Damage			μ_{Δ}
		Δ_y /mm	P_y /kN	θ_y	Δ_u /mm	P_u /kN	θ_u	Δ_d /mm	P_d /kN	θ_d	
SRHSC1-B0	Push	9.2	219.7	1/116	15.4	254.7	1/75	24.5	216.5	1/41	2.67
	Pull	-8.1	-201.7		-11.3	-237.5		-24.6	-201.8		3.05
SRHSC1-B1	Push	7.9	166.4	1/123	12.5	190.6	1/81	17.5	162.0	1/59	2.22
	Pull	-8.4	-186.6		-12.2	-213.9		-23.4	-181.8		2.78
SRHSC1-B2	Push	6.2	183.2	1/144	9.9	205.0	1/90	13.6	174.3	1/57	2.19
	Pull	-7.6	-109.5		-12.3	-130.2		-21.4	-110.7		2.80
SRHSC1-B3	Push	7.5	127.1	1/132	10.2	149.5	1/97	16.6	127.1	1/58	2.23
	Pull	-7.7	-139.4		-10.4	-156.4		-17.9	-132.9		2.32
SRHSC2-B0	Push	10.7	211.2	1/94	13.6	243.5	1/62	30.2	206.9	1/33	2.83
	Pull	-10.5	-191.5		-18.8	-228.2		-29.6	-194.0		2.82
SRHSC2-B1	Push	7.9	183.4	1/128	15.1	217.3	1/81	23.6	184.7	1/45	2.97
	Pull	-7.6	-155.8		-9.8	-186.9		-21.0	-158.9		2.75
SRHSC2-B2	Push	9.3	207.9	1/116	12.1	231.2	1/99	19.1	196.5	1/47	2.06
	Pull	-7.9	-81.9		-8.1	-99.2		-23.1	-84.3		2.93
SRHSC2-B3	Push	8.0	159.2	1/120	11.3	193.4	1/73	15.2	164.4	1/54	1.90
	Pull	-8.6	-119.7		-16.3	-133.9		-22.0	-113.8		2.55

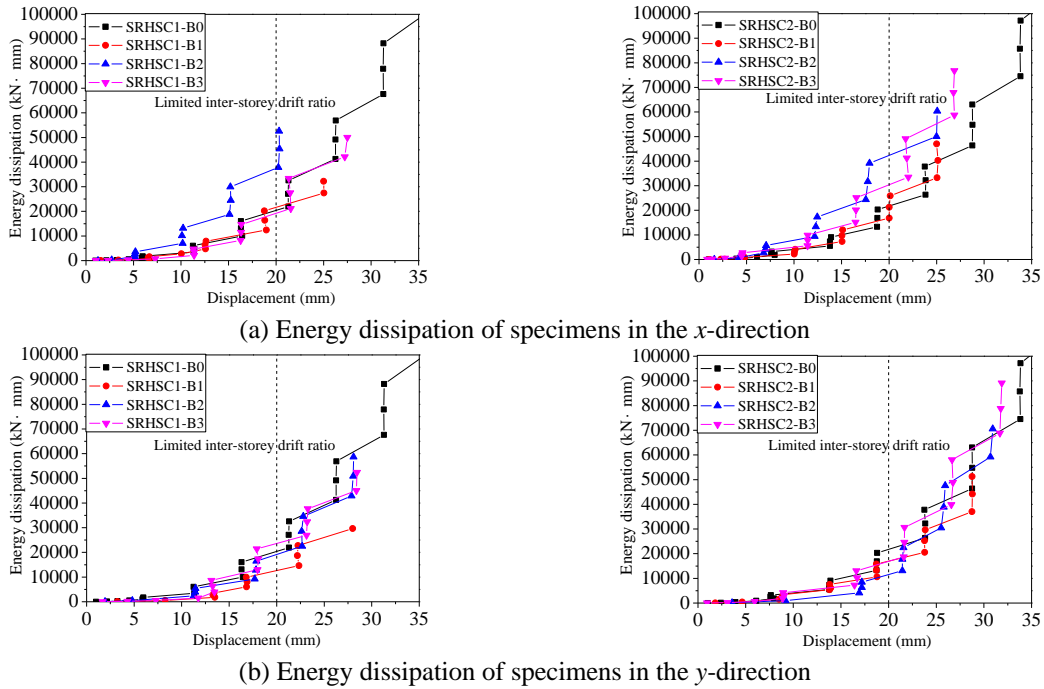


Fig. 8 Comparison of energy dissipation of specimens under various loading paths

Table 6 Energy dissipation of specimens subjected to various loading paths

Various loading stage	Specimen	x-direction		y-direction		Energy dissipation ratio	
		Disp. (mm)	Energy dissipation (kN · mm)	Disp. (mm)	Energy dissipation (kN · mm)	$\frac{E_{xb}}{E_{xu}}$	$\frac{E_{xb} + E_{yb}}{E_{xu}}$
Damage disp.	SRHSC1-B0	24.55	38506	-	-	-	-
	SRHSC1-B1	20.45	22320	23.25	24027	0.58	1.20
	SRHSC1-B2	17.5	33827	23.85	35950	0.88	1.81
	SRHSC1-B3	17.25	15933	23.55	38095	0.41	1.40
	SRHSC2-B0	29.9	65758	-	-	-	-
	SRHSC2-B1	22.3	28706	24.45	30824	0.44	0.91
	SRHSC2-B2	21.1	44039	22.95	25734	0.67	1.06
	SRHSC2-B3	18.6	28294	24.05	35092	0.43	0.96
1/50	SRHSC1-B0	20	20202	-	-	-	-
	SRHSC1-B1	20	21466	20	12519	1.06	1.68
	SRHSC1-B2	20	37653	20	19348	1.86	2.82
	SRHSC1-B3	20	19348	20	23584	0.96	2.13
	SRHSC2-B0	20	21466	-	-	-	-
	SRHSC2-B1	20	26145	20	17198	1.22	2.02
	SRHSC2-B2	20	42332	20	11666	1.97	2.52
	SRHSC2-B3	20	30413	20	17198	1.42	2.22

for SRHSC1-B1, SRHSC1-B2 and SRHSC1-B3, respectively. It indicates that biaxial loading could decrease the damage drift ratio significantly. And it also demonstrates that identical SRHSC columns under uniaxial loading meet the limited inter-storey drift ratio 1/50 specified in Chinese code (2010), but it doesn't meet the requirement when subjected to bidirectional loading. As for ductility coefficient, they were reduced by an average of 15.20% and 10.56% for specimen group SRHSC1 and SRHSC2 when subjected to biaxial loading. Thus, the effect of bi-directional earthquake actions on deformation capacity of structures should not be ignored in the structure design.

3.5 Energy dissipation capacity

Energy dissipation capacity is an important seismic performance index for structure or structure member, which is represented by cumulative energy dissipation in this paper. The cumulative energy dissipation of test specimens obtained from test is shown in Fig. 8, where the limited inter-storey drift ratio specified in Chinese code (2010) is 1/50, and the corresponding lateral displacement is 20 mm for this test specimen. Before yielding lateral load was attained, energy dissipation was so small that it was neglected in the computation of energy dissipation. From

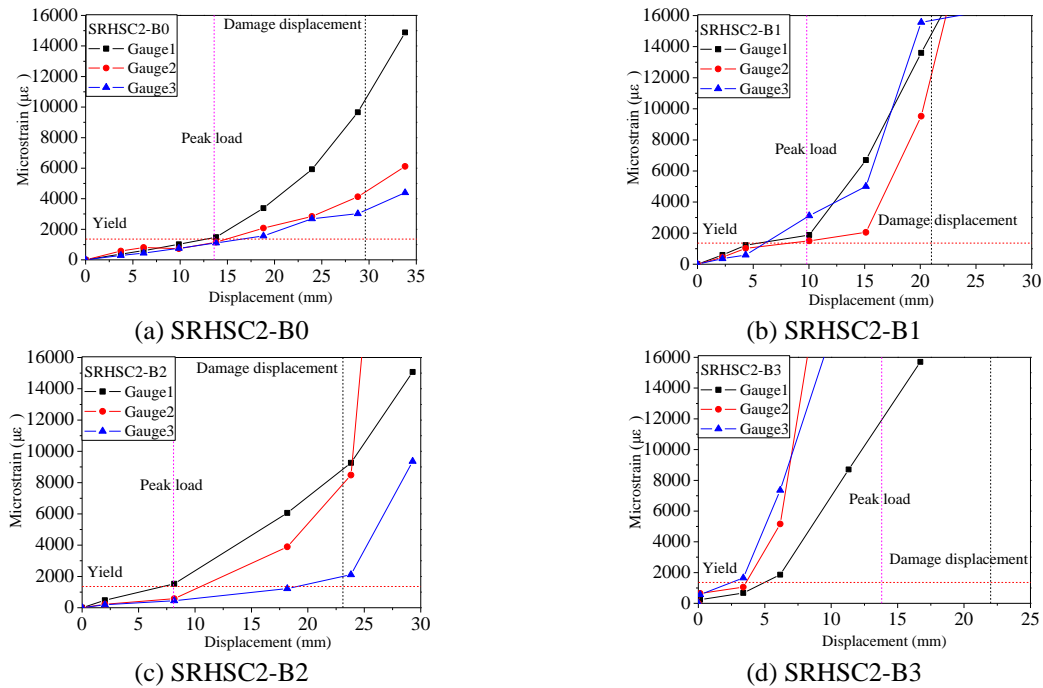


Fig. 9 Strain of steel for specimens

(Note: strain value in Fig. 9 is the maximum strain value of the gauge readings in the same layer)

Fig. 8, it can be seen that the x -direction cumulative energy dissipation from bidirectional cyclic loaded specimen was close to or larger than the one of specimen under uniaxial loading during the same displacement loading. However, the y direction cumulative energy dissipation of specimens SRHSC1 and SRHSC2 subjected to biaxial cyclic loading was close to or smaller than those under uniaxial cyclic loading during the same displacement loading level.

Energy dissipation of specimen is influenced by loading paths significantly. To make a clear comparison, the cumulative energy dissipation from specimens loaded to various stage and their ratios are tabulated in Table 6, where ‘Damage disp.’ represents ‘Damage displacement’ for short. The damage displacement is defined as the one where 85% of peak lateral load is sustained. ‘ E_{xu} ’ stands for energy dissipation of specimens subjected to uniaxial loading, while ‘ E_{xb} ’ and ‘ E_{yb} ’ represent x - and y -direction energy dissipation of bidirectional loaded specimen, respectively.

What could be seen from Table 6 was that, when loaded to the damage displacement, x -direction energy dissipation from biaxially loaded specimen was smaller than that of specimen under unidirectional loading. The energy dissipation ratio was ranging from 0.41 to 0.88. However, the total energy dissipation of specimen in the two loading directions was approximately equal to or larger than that of specimen subjected to unidirectional cyclic loading that all depended on the biaxial loading pattern. The energy dissipation ratio was ranging from 0.91 to 1.81. When loaded to the limited inter-storey drift ratio (1/50), except for specimen SRHSC1-B3 (the energy dissipation ratio was 0.96), other x -direction energy dissipations were all larger than energy dissipations of uniaxially loaded specimens, having a ratio ranging from 1.68 to 2.82.

The results above indicates that loading path has

significant influence on the energy dissipation, and energy dissipation of specimens subjected to various bidirectional loading differed greatly. Energy dissipation capacity of specimens subjected to biaxial cyclic loading had a better development than those under uniaxial cyclic loading.

3.6 Strain of reinforcement

3.6.1 Strain of steel

Fig. 9 shows the development of strains in steel at various drift ratios for specimens. Strain gauge readings indicate that steel could reach yielding strength during the test. At the same time, it can be seen that the development of steel strain is closely related to loading paths. Gradual increase of steel strain was observed in the specimen under loading path B0, while steel strain was increasing sharply as drift ratio increased in specimens subjected to loading paths B1, B2 and B3, especially after the yielding of steel. When loaded to the limited inter-storey drift ratio 1/50 specified in Chinese code (the corresponding lateral displacement is 20mm for this test), steel strain was 0.0040 for specimen under unidirectional loading path B0, while steel strains were 0.0154 and 0.0071 for specimens under bidirectional loading path B1 and B2, and they were 3.85 and 1.78 times as large as the former. As loaded to a lateral drift of 20mm, steel strain in specimen SRHSC2-B3 was too large and strain gauges were in failure, so steel strain was not given in the paper. Results indicate that steel strain of specimens under biaxial loading is much larger than those under uniaxial loading.

Furthermore, yielding drifts of specimens under various loading paths differs greatly. Yielding drift is smaller in specimens under bidirectional loading than those subjected to unidirectional loading. For the set of identical specimens

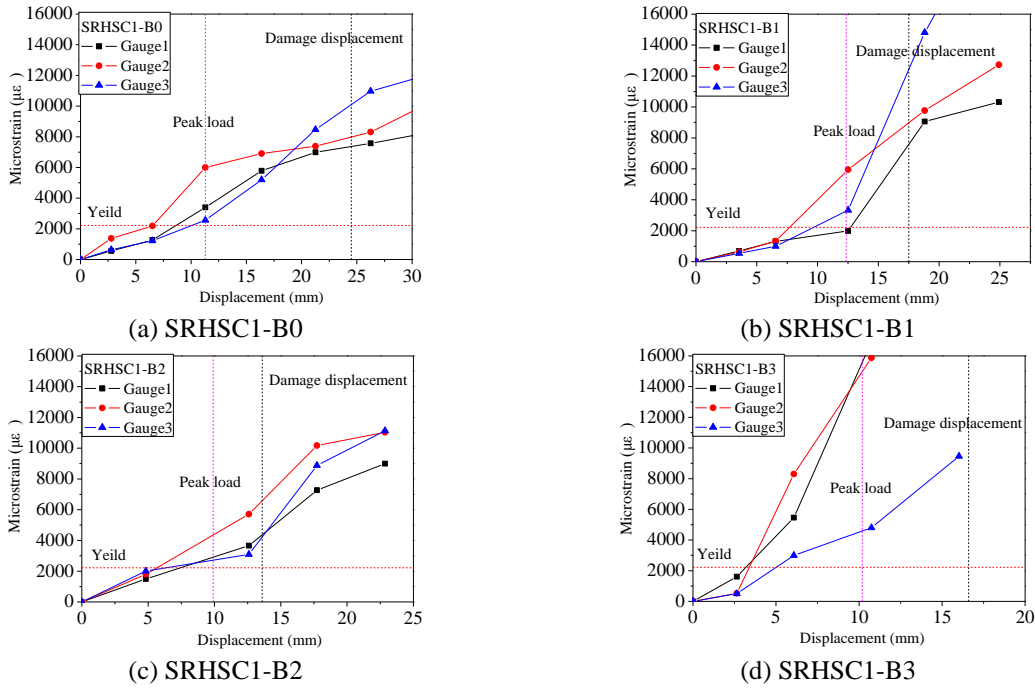


Fig. 10 Strain of longitudinal steel bars for specimens
(Note: strain value in Fig. 10 is the maximum strain value of the gauge readings in the same layer)

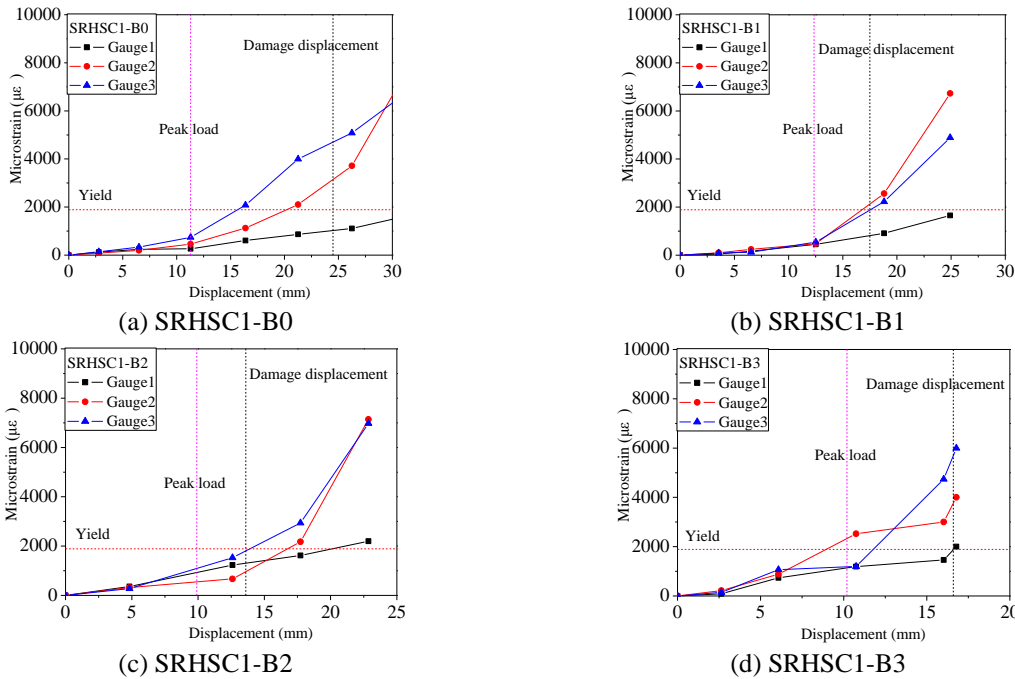


Fig. 11 Strain of stirrups for specimens
(Note: strain value in Fig. 11 is the maximum strain value of the gauge readings in the same layer)

SRHSC2, the yielding displacement was 13.5 mm in the uniaxial loading condition B0, while the yielding drifts were 6 mm, 7.5 mm and 3.4 mm under biaxial loading paths B1, B2 and B3, respectively. Correspondingly, the yielding displacements were decreased by 55.56%, 44.44% and 74.81% under loading paths B1, B2 and B3, respectively.

3.6.2 Strain of longitudinal reinforcing bars

Strains of longitudinal reinforcing bars for the set of

specimen SRHSC1 are shown in Fig. 10. From Fig. 10, it is noted that the strain development of longitudinal reinforcing bars is similar with that of steel. Strain of longitudinal reinforcing bars in biaxially loaded specimen grew faster than that in the uniaxially loaded specimen, hence, specimens got a little yielding drift under bidirectional loading. For the set of identical specimen SRHSC1, the yielding lateral drifts were 6.5 mm, 7.6 mm, 5.7 mm and 3.2 mm for specimens subjected to loading path

B0, B1, B2 and B3, respectively. This might be because that corner steel bar is more far away from the neutral axis under loading paths B2 and B3 than other loading conditions. As the lateral drift increased, stress of corner longitudinal reinforcement grew more fast than that of other longitudinal steel bars, so they had a smaller yielding displacement. After yielding, strain of longitudinal reinforcement grew fast and fast in specimen under loading path B3. And the stress was 2-3 times as large as that of specimens under other loading paths. As loaded to the limited inter-storey drift ratio 1/50, strain grew to 0.0077, 0.0165 and 0.0106 for specimen SRHSC1-B0, SRHSC1-B1 and SRHSC1-B2, respectively. Correspondingly, strains in specimen SRHSC1-B1 and SRHSC1-B2 were 2.14 and 1.38 times as large as the one in specimen SRHSC1-B0. Since strain gauges had been in failure at the inter-storey drift ratio 1/50, strain in specimen SRHSC1-B3 was not given here. The result demonstrates that loading path had a significant effect on the stress development of longitudinal reinforcement.

3.6.3 Strain of transverse reinforcing bars

Stirrup stress level can reflect the restraint condition of core concrete, also it is an important index in designing earthquake resistant members and structures. Fig. 11 only gives the strain development of transverse reinforcing bars of specimen group SRHSC1, since a similar strain development is obtained in specimen group SRHSC2. Noticed that stirrup strain grew slowly at the beginning of the test loading. However, strain increased fast and fast in subsequent loading, especially after the peak load was attained. When loaded to the peak load, there were no yielding of stirrups observed in specimen SRHSC1-B0, SRHSC1-B1 and SRHSC1-B2. And the maximum strains were about 7.71×10^{-4} , 5.35×10^{-4} and 1.01×10^{-3} , which were approximately 40%, 28% and 58% of the yielding strain, respectively. Stirrup from specimen SRHSC1-B3 had reached yielding at the peak load, and the maximum strain was 2.34×10^{-3} , which was 1.24 times of the yielding strain correspondingly. As loaded to the damage displacement, transverse reinforcement of specimen SRHSC1-B1 and SRHSC1-B2 had reached or been close to the yielding strength, while most stirrups from specimen SRHSC1-B3 had already happened to yielding earlier, and the strain was 3.03 times as large as yielding strain of stirrup.

4. Conclusions

An experimental program was carried out on eight SRHSC columns subjected to a combination of constant axial load and uniaxial or biaxial cyclic lateral load. The seismic performance of specimens was discussed. In general, the experimental results show that behavior of the SRHSC columns is highly dependent on the loading pattern. The conclusions can be drawn as follows:

- With a same steel ratio, deformation capacity of SRHSC columns with square steel tubular is superior to the one with cross-shape steel, and the yielding drift ratio and ultimate drift ratio are increased by 23.40% and 24.24%, respectively.

- Loading path affects hysteretic character of specimens significantly. Hysteretic character exhibits evident asymmetry for specimens subjected to asymmetric loading, like B2 for example.

- By contrast with specimens under uniaxial loading, SRHSC columns subjected to biaxial loading possess low carrying capacity, fast stiffness degradation, small yielding drift and poor deformation capacity. Positive and negative peak load are decreased by an average of about 15%-35%, it all depends on the form of biaxial loading. Displacement ductility ratio is reduced by 10%~15%, while damage drift ratio is decreased by 30% approximately.

- Generally, yielding of longitudinal reinforcement happens before the peak load is attained, while steel happens to yielding when loaded to the peak strength. Moreover, strain of steel and longitudinal reinforcing bars increases gradually in specimens under unidirectional loading, while it grows sharply in specimens subjected to bidirectional loading, especially after yielding of steel and longitudinal reinforcement.

Thus, effect of bi-directional earthquake actions on seismic behavior of members or structures should be paid more attention in structure design.

Acknowledgments

The authors would like to thank National Natural Science Foundation of China (Grant NO. 51608434, 51478382 and 51668007) and Natural Science Foundation Research Project of Shaanxi province (Grant NO. 2016JQ5082) for their generous financial support of this research work. Technical assistance and cooperation of the laboratory staff are greatly appreciated.

References

- Ahmad, S.H. and Weerakoon, S.L. (1995), "Model for behavior of slender reinforced concrete columns under biaxial bending", *ACI Struct. J.*, **92**(2), 188-198.
- Bechtoula, H., Kono, S. and Watanabe, F. (2005), "Experimental and analytical investigations of seismic performance of cantilever reinforced concrete columns under varying transverse and axial loads", *J. Asian Arch. Build. Eng.*, **4**, 467-474.
- Bousias, S.N., Verzeletti, G., Fardis, M.N. and Gutierrez, E. (1995), "Load-path effects in column biaxial bending with axial force", *J. Eng. Mech.*, **121**, 596-605.
- Chang, S.Y. (2010), "Experimental studies of reinforced concrete bridge columns under axial load plus biaxial bending", *J. Struct. Eng.*, **136**(1), 12-25.
- de Sousa Jr, J.B. and Caldas, R.B. (2005), "Numerical analysis of composite steel-concrete columns of arbitrary cross section", *J. Struct. Eng.*, **131**(11), 1721-1730.
- Dundar, C., Tokgoz, S., Tanrikulu, A.K. and Baran, T. (2008), "Behaviour of reinforced and concrete-encased composite columns subjected to biaxial bending and axial load", *Build. Environ.*, **43**(6), 1109-1120.
- Farah, A. and Huggins, M.W. (1969), "Analysis of reinforced concrete subjected to longitudinal load and biaxial bending", *ACI J.*, **66**(7), 569-575.
- Furlong, R.W. (1979), "Concrete columns under biaxial eccentric

- thrust”, *ACI J.*, **76**(10), 1093-1118.
- GB 50011-2010, (2010), Code for Seismic Design of Buildings, Beijing.
- Germano, F., Tiberti, G. and Plizzari, G. (2016), “Experimental behavior of SFRC columns under uniaxial and biaxial cyclic loads”, *Compos. Part B*, **85**, 76-92.
- Hong, H.P. (2000), “Short reinforced concrete column capacity under biaxial bending and axial load”, *Can. J. Civil. Eng.*, **27**, 1173-1182.
- Hong, H.P. (2001), “Strength of slender reinforced concrete columns under biaxial bending”, *J. Struct. Eng.*, **127**(7), 758-762.
- Hsu, C.T.T. (1985), “Biaxially loaded L-shaped reinforced concrete columns”, *J. Struct. Eng.*, **111**(12), 2576-2595.
- Hsu, C.T.T. (1989), “T-shaped reinforced concrete members under biaxial bending and axial compression”, *ACI Struct. J.*, **86**(4), 460-468.
- Kang, H.Z. and Jiang, J.J. (2003), “Experiment study on seismic behavior of RC frame columns under varied loading paths”, *Chin. Civil Eng. J.* **36**(5), 71-75.
- Kozinski, K. and Winnicki, A. (2016), “Experimental research and analysis of load capacity and deformability of slender high strength concrete columns in biaxial bending”, *Eng. Struct.*, **107**, 47-65.
- Mavichak, V. and Furlong, R.W. (1976), “Strength and stiffness of reinforced concrete columns under biaxial bending”, Res. Rep. 7-2F, Ctr. for Hwy. Res., University of Texas at Austin, Austin.
- Muñoz, P.R. and Hsu, C.T.T. (1997), “Behavior of biaxially loaded concrete-encased composite columns”, *J. Struct. Eng.*, **123**, 1163-1171.
- Otani, S., Cheung, V.M.T. and Lai, S.S. (1977), “Reinforced concrete columns subjected to biaxial lateral load reversals”, *Proceedings of the 6th World Conference on Earthquake Engineering*, New Delhi, India, January.
- Poston, R.W., Breen, J.E. and Roesset, J.M. (1985a), “Analysis of nonprismatic or hollow slender concrete bridge piers”, *ACI J.*, **82**(5), 731-739.
- Poston, R.W., Gilliam, T.E., Yamamoto, Y. and Breen, J.E. (1985b), “Hollow concrete bridge pier behavior”, *ACI J.*, **82**(6), 779-787.
- Qiu, F.W., Li, W.F., Pan, P. and Qian, J. (2002), “Experimental tests on RC columns under biaxial quasi-static loading”, *Eng. Struct.*, **24**, 419-428.
- Quang, K.M., Dang, V.B.P., Han, S.W., Shin, M. and Lee, K. (2016), “Behavior of high-performance fiber-reinforced cement composite columns subjected to horizontal biaxial and axial loads”, *Constr. Build. Mater.*, **106**, 89-101.
- Rodrigues, H., Arêde, A., Varum, H. and Costa, A.G. (2013b), “Experimental evaluation of rectangular reinforced concrete column behaviour under biaxial cyclic loading”, *Earthq. Eng. Struct. D.*, **42**, 239-259.
- Rodrigues, H., Arêde, A., Varum, H. and Costa, A.G. (2013c), “Damage evolution in reinforced concrete columns subjected to biaxial loading”, *B. Earthq. Eng.*, **11**, 1517-1540.
- Rodrigues, H., Furtado, A. and Arêde, A. (2016), “Behavior of rectangular reinforced-concrete columns under biaxial cyclic loading and variable axial loads”, *J. Struct. Eng.*, **142**(1), 04015085.
- Rodrigues, H., Romão, X., Campos, A.A., Varum, H., Arêde, A. and Costa, A.G. (2012b), “Simplified hysteretic model for the representation of the biaxial bending response of RC columns”, *Eng. Struct.*, **44**, 146-158.
- Rodrigues, H., Varum, H., Arêde, A. and Costa, A.G. (2012a), “A comparative analysis of energy dissipation and equivalent viscous damping of RC columns subjected to uniaxial and biaxial loading”, *Eng. Struct.*, **35**, 149-164.
- Rodrigues, H., Varum, H., Arêde, A. and Costa, A.G. (2013a), “Behaviour of reinforced concrete column under biaxial cyclic loading-state of the art”, *Adv. Struct. Eng.*, **5**(4), 1-12.
- Sayed, M.E. and Maaddawy, T.E. (2011), “Analytical model for prediction of load capacity of RC columns confined with CFRP under uniaxial and biaxial eccentric loading”, *Mater. Struct.*, **44**, 299-311.
- Tokgoz, S. and Dundar, C. (2008), “Experimental tests on biaxially loaded concrete-encased composite columns”, *Steel Compos. Struct.*, **8**(5), 423-438.
- Tsuno, K. and Park, R. (2004), “Experimental study of reinforced concrete bridge piers subjected to bi-directional quasi-static loading”, *Eng. Struct.*, **21**(1), 11-26.
- Ucak, A. and Tsopelas, P. (2015), “Load path effects in circular steel columns under bidirectional lateral cyclic loading”, *J. Struct. Eng.*, **141**(5), 1-11.
- Wang, G.G. and Hsu, C.T.T. (1992), “Complete biaxial load-deformation behavior of RC columns”, *J. Struct. Eng.*, ASCE, **118**(9), 2590-2609.
- Wang, G.G. and Hsu, C.T.T. (1998), “Nonlinear analysis of reinforced concrete columns by cubic-spline function”, *J. Eng. Mech.*, ASCE, **124**(7), 803-810.
- Warner, R.F. (1969), “Biaxial moment thrust curvature relation”, *J. Struct. Div.*, ASCE, **95**(5), 923-940.

CC